Transient Hydromagnetic Maxwell Fluid Flow over Inclined Stretching Surface with Thermal Radiation, Viscous Dissipation and Ohmic Heating Effects

Abiodun A. Opanuga (abiodun.opanuga@covenantuniversity.edu.ng)
Covenant University
Olasunmbo O. Agboola
Covenant University
Hilary I. Okagbue
Covenant University
Ibikunle Olajide
Gateway (ICT) Polytechnic

Research Article

Keywords: Transient flow, stretching surface, Maxwell fluid, magnetohydrodynamic (MHD), thermal radiation, Runge-Kutta method.

Posted Date: September 29th, 2023

DOI: https://doi.org/10.21203/rs.3.rs-3379582/v1

Additional Declarations: No competing interests reported.

Transient Hydromagnetic Maxwell Fluid Flow over Inclined Stretching Surface with Thermal Radiation, Viscous Dissipation and Ohmic Heating Effects

Abiodun A. Opanuga[a*], Olasunmbo O. Agboola[a], Hilary I. Okagbue[a], Ibikunle Olajide[b]

[a]*Department of Mathematics, Covenant University, Ota, Ogun State, 112104, Nigeria*
[b]*Department of Mathematics and Statistics, Gateway (ICT) Polytechnic, Saapade, Ogun State, 121104, Nigeria*

Abstract: Analysis of an electrically conducting two-dimensional Maxwell fluid flowing through an inclined stretching sheet is considered in this work. Incorporating the viscous dissipation and Ohmic heating effects on the time-dependent optically dense fluid, and using the required similarity transformation variables, the equations governing the flow are deduced and converted into a coupled system of ordinary differential equations. Runge-Kutta fourth order scheme with shooting technique is applied to solve the derived equations. Plots and tables are employed to explain the flow parameters for fluid velocity, temperature, and concentration profiles as well as the skin friction, local Nusselt number, and local Sherwood number. Increase in the angle of inclination parameter, Hartmann number, Prandtl number and Schmidt number reduce the magnitude of the fluid velocity, while radiation parameter, Grashof and Eckert numbers increase it. However, fluid temperature is significantly moderated by Grashof and Prandtl numbers.

Keywords: Transient flow, stretching surface, Maxwell fluid, magnetohydrodynamic (MHD), thermal radiation, Runge-Kutta method.

Introduction

In recent years, the dynamics of non-Newtonian fluids have received considerable attention due to their divergent areas of applications, such as in biological sciences, medical sciences, geophysics, chemical and petroleum industries. The non-linearity ratio between the shear stress and shear rate distinguishes non-Newtonian fluid from Newtonian fluid. In addition, it possesses more complex rheological properties than Newtonian fluid models. Numerous industrially important fluids captured as non-Newtonian are molten plastics, polymers, pulps, mud, pasta, personal care products, ice cream, paints, oils, cheese, asphalt, etc. Due to the complexity of the rheological properties of non-Newtonian fluids, Navier-Stokes' equation has difficulty capturing their mathematical models. Hence, several mathematical models have been developed to account for the divergent features of these fluids. A few of these features include shear thinning, shear thickening, yield stress, stress relaxation etc. The power law model is usually applied to exhibit both the shear thinning and shear thickening effects, the yield stress is addressed by Casson fluid model and the elasticity effect is modeled by grade fluids. Others are micropolar stagnation flows (Odelu and Naresh [1]), Walter's viscoelastic flows (Hussain and Ullah [2]), Jeffrey's viscoelastic boundary layers (Gaffar et al.[3]), Williamson fluids (Megahed.[4]), nanofluid transport from a sphere (Prasad et al. [5]), Eyring–Powell fluid (Gaffar et al. [6]), tangent hyperbolic fluid (Gaffar et al.[7]), and Jeffery nanofluid (Mehmood et al. [8]).

However, these models do not address the effects of stress relaxation, and because a rate-type fluid subclass known as the Maxwell model can predict stress relaxation, it has gained prominence. This model also eradicates the complex impacts of shear-dependent viscosity, making it ideal for concentrating on the effects of a fluid's elasticity on the features of its boundary. Aliakbar et al. [9] investigated the effect of thermal radiation on MHD Maxwell fluid flow over a stretching surface. The effects of thermal radiation and Joule heating on the MHD flow of Maxwell fluid above a stretching sheet were examined by Hayat and Qasim [10]. Heat transfer analysis of time-dependent Maxwell fluid flow over a stretching sheet was studied by Mukhopadhyay [11]. Furthermore, the impact of mass transfer on the Maxwell fluid flow passing through an unsteady stretching sheet was discussed by Mukhopadhyay and Bhattacharyya [12].

Meanwhile, investigations into fluid flow over a stretching surface have experienced a surge in recent decades as a result of its diverse industrial and technological applications, such as metal formation (Altan et al.[13]), polymer extrusion (Fisher [14]) and drawing of plastic films (Tadmor and Klein [15]). Others are metal spinning, glass-fibre production, solidification of liquid crystals, paper production, petroleum production, exotic lubricants and suspension solutions. Crane [16] initiated the stretching surface flows and obtained the closed form solution of viscous flow over a linearly stretching surface. Cane's work has since been addressed by a number of researchers in a bid to incorporate various aspects of fluid flows and flow configurations. Ishak [17] considered the effect of unsteadiness. Grubka and Bobba [18] studied the impact of variable temperature. Sharidan et al. [19] obtained the similarity solutions for the unsteady boundary layer flow. Chamkha et al. [20] considered porosity, suction/injection and chemical reaction effects, while Eldabe et al. [21] considered three-dimensional flow over a stretching surface. Yusuf et al. [22] investigated Williamson nanofluid over a stretching surface with chemical reaction. Mustafa et al. [23] analysed the unsteady boundary layer flow of a Casson fluid.

It is worth mentioning that interest in the investigation of thermal radiation effect in a stretching sheet has grown rapidly in the last few decades; due to its relevance in the design of critical equipment such as fins, ceramic and glass manufacturing units, and various propulsion devices for aircraft, missiles, satellites, and space vehicles. In view of the aforementioned applications, Rosseland [24] developed the optically thick approximation for radiation flux. Thereafter, several researchers have since incorporated it into various fluid flows. Hossain and Takhar [25] presented radiation effects on mixed convection flow, and Hossain et al. [26] studied the effect of radiation on free convection from a vertical porous plate. Furthermore, Hossain et al. investigated the effect of radiation on free convection flow. Bataller [27] analysed the radiation effects on the Blasius and Sakiadis flows. Sajid and Hayat [28] investigated the effect of thermal radiation on the boundary layer flow. Gbadeyan and Yusuf [29] examined the effect of nonlinear partial slip and thermal radiation on Oldroyd 8 - constant fluid, and thermal radiation effect on hydromagnetic steady asymmetric flow was considered by Makinde [30].

Despite the numerous benefits of viscous effect in several fields like tribology, instrumentation, food processing, lubrication, polymer manufacturing, etc., it has not been taken into account by several researchers in a variety of hydromagnetic heat and mass transfer flows. However, many fluids' viscosities, vary with temperature. For instance, the viscosity of dry air is 21.94 x 10-6 kg/ms at 100°C and 26.94 x 10-6 kg/ms at 200°C. As a result, it is inappropriate to ignore these vital impact when analyzing fluid flows since doing so could give rise to conclusions that are either under-or over-determined, depending on the situation from using constant viscosity. In view of its significance, Vajravelu and Hadjinicolaou [31] analyzed boundary layer flow over a stretching sheet, taking viscous dissipation into account. Partha et al. [32] examined viscous dissipation effect on the mixed convection flow with heat transfer over an exponentially stretching surface. Sanjayanand and Khan [33] discussed viscous dissipation effect on boundary layer fluid flow over an exponentially stretching surface. Cortell [34] considered the effects of viscous dissipation and thermal radiation on boundary layer flow over a non-linearly stretching sheet. Aziz [35] studied viscous dissipation effect on micropolar fluid over an exponentially stretching sheet. Pavithra and Gireesha [36] presented the effect of viscous dissipation on hydromagnetic fluid flow in a porous medium.

An Ohmic heating (Joule heating) effect is produced when an electrically conducting fluid interacts with an externally applied magnetic field. In other words, it is a process that produces heat when an electric current flows through a conductor. Ohmic heating is used in a variety of industrial and technological processes, which include electric stoves, heaters, incandescent light bulbs, electric fuses, electronic cigarettes, thermistors, food processing, and many others. Devi and Ganga [37] have considered the impacts of viscous and Ohmic heating on hydromagnetic flow problem. Megahed [38] research work considered joule heating and viscous dissipation on magnetohydrodynamic flow past a stretching sheet, and recently, Swain et al. [39] studied viscous dissipation and joule heating effect on hydromagnetic flow past a porous stretching surface. Others are Muhammad et al. [40], Adegbie et al. [41], Osalusi et al. [42], Goud and Nandeppanavar [43], Hasan et al. [44] and Gireesha et al. [45].

The current analysis focuses on the investigation of thermal radiation, viscous dissipation, and Ohmic heating effects on transient hydromagnetic Maxwell fluid over an inclined stretching surface. The findings of this research will be immensely beneficial in the industry for engineers and scientists to boost the efficiency of Maxwell fluid flow during industrial processes.

Description of Model

Consider a two-dimensional incompressible transient hydromagnetic Maxwell fluid over a stretched surface inclined from the vertical with the inclination angle γ, which is coinciding with the plane $y=0$. It is assumed that at $t<0$ the flows are steady, however the unsteady heat and mass flows begin at $t=0$ with the velocity $U(x,t)=cx/(1-\alpha t)$, such that c and α are positive constants with dimensions $(\text{time})^{-1}$. Note that c and $c/(1-\alpha t)$ are the initial stretching and effective stretching rates respectively and are increasing with time. Further assumption is that, a magnetic field with constant strength B_0 is applied in the direction normal to the flow direction, as depicted in Figure 1. The flow is induced by the stretching of the sheet, due to the application of two equal and opposing forces simultaneously along the x-axis. Keeping the origin constant, the sheet is stretched with a speed that varies linearly with distance from the slit. $T_w(x,t)$ and $C_w(x,t)$ are the sheet surface temperature and concentration respectively while the constants free stream temperature and concentration are T_∞ and C_∞ respectively, such that $T_w>T_\infty$ and $C_w>C_\infty$. It is assumed that both $T_w(x,t)$ and $C_w(x,t)$ vary along the sheet and with time as $T_W(x,t)=T_\infty+bx(1-\alpha t)^{-2}$, and $C_W(x,t)=C_\infty+bx(1-\alpha t)^{-2}$.

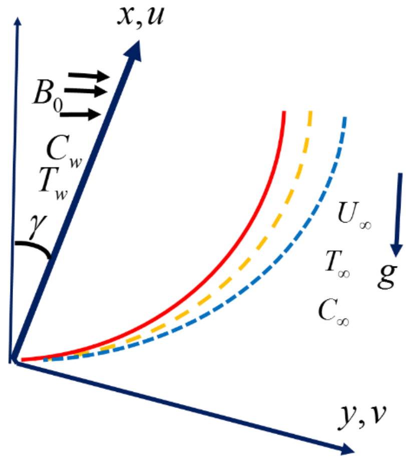

Fig. 1: Flow Configuration

Under the aforementioned assumptions, the boundary layer equations of a Maxwell fluid can be stated as (Mukhopadhyay [11]; Mukhopadhyay and Bhattacharyya [12]):

$$\frac{\partial u}{\partial x}+\frac{\partial v}{\partial y}=0 \tag{1}$$

$$\begin{aligned}\frac{\partial u}{\partial t}+u\frac{\partial u}{\partial x}+v\frac{\partial u}{\partial y}&=\upsilon\frac{\partial^2 u}{\partial y^2}-\frac{\sigma B_0^2}{\rho}\left(u+\lambda v\frac{\partial u}{\partial y}\right)\\&+\lambda\left(u^2\frac{\partial^2 u}{\partial x^2}+v\frac{\partial^2 u}{\partial y^2}+2uv\frac{\partial^2 u}{\partial x\partial y}\right)\\&+g\left[\beta_T(T-T_\infty)+\beta_C(C-C_\infty)\right]\cos\gamma\end{aligned} \tag{2}$$

$$\frac{\partial T}{\partial t}+u\frac{\partial T}{\partial x}+v\frac{\partial T}{\partial y}=\alpha_c\frac{\partial^2 T}{\partial y^2}+\frac{1}{\rho C_p}\frac{\partial q_r}{\partial y}+\frac{\mu}{\rho C_p}\left(\frac{\partial u}{\partial y}\right)^2+\frac{\sigma B_0^2 u^2}{\rho C_p} \tag{3}$$

$$\frac{\partial C}{\partial t}+u\frac{\partial C}{\partial x}+v\frac{\partial C}{\partial y}=D\frac{\partial^2 T}{\partial y^2} \tag{4}$$

Since the modelled Maxwell fluid is flowing past a stretching surface, the appropriate boundary conditions are:

$$\left.\begin{aligned}&u=U_w, v=0, T=T_w, C=C_w \text{ at } y=0\\&u\to 0, T\to T_\infty, C\to C_\infty \text{ at } y\to\infty\end{aligned}\right\} \tag{5}$$

Note that in the expression above, u and v are fluid velocity components along $x-$axis and $y-$axis respectively.
Introducing the Rosseland approximation for the radiative heat flux which appears in the energy equation as

$$q_r = -\frac{4\sigma^c}{3k^c}\frac{\partial T^4}{\partial y} = -\frac{16\sigma^c T^3}{3k^c}\frac{\partial T}{\partial y}. \tag{6}$$

In Eq. (6), T is highly non-linear in the energy equation which makes its solution very difficult, hence an assumption of small temperature differences within the flow is taken which helps to linearize the Rosseland formula about the ambient temperature T_∞. This means T^3 in Eq. (6) is substituted with T_∞^3.
Invoking Eq. (6) in Eq. (3) yields

$$\frac{\partial T}{\partial t} + u\frac{\partial T}{\partial x} + v\frac{\partial T}{\partial y} = \alpha_c\frac{\partial^2 T}{\partial y^2} + \frac{16\sigma^c T_\infty^3}{3\rho C_p k^c}\frac{\partial^2 T}{\partial y^2} + \frac{\mu}{\rho C_p}\left(\frac{\partial u}{\partial y}\right)^2 + \frac{\sigma B_0^2 u^2}{\rho C_p} \tag{7}$$

The following relations are introduced for u, v, θ and ϕ **:**

$$u = \frac{\partial \psi}{\partial y},\ v = -\frac{\partial \psi}{\partial x},\ \theta = \frac{T - T_\infty}{T_w - T_\infty},\ \phi = \frac{C - C_\infty}{C_w - C_\infty} \tag{8}$$

where ψ is a stream function. Furthermore, the following similarity transformation variables are introduced

$$\eta = \sqrt{\frac{c}{v(1-\alpha t)}}\,y,\ \psi = \sqrt{\frac{vc}{(1-at)}}\,xf(\eta),\ T_w = T_\infty + \frac{cx}{(1-\alpha t)^2}\theta(\eta),\ C_w = C_\infty + \frac{cx}{(1-\alpha t)^2}\phi(\eta) \tag{9}$$

Employing the relations (9), converts Eqs. (2), (4) and (7) to the following system of coupled ordinary differential equations

$$f''' + ff'' - (f')^2 + A\left(\frac{\eta}{2}f''' + f'\right) - \beta\left(f^2 f''' - 2fff''\right) - Ha^2\left(f' + \beta ff''\right) - \left(Gr\theta + Gc\phi\right)\cos\gamma = 0 \tag{10}$$

$$\frac{1}{\Pr}(1 + Nr)\theta'' + f\theta' - f'\theta - A\left(\frac{\eta}{2}\theta' + \theta\right) + Ec(f'')^2 + EcHa^2(f')^2 = 0 \tag{11}$$

$$\frac{1}{Sc}\phi + f\phi' - f'\phi - A\left(\frac{\eta}{2}\phi' + \phi\right) = 0 \tag{12}$$

Then the boundary conditions in (5) take the form

$$f(0)=0, f'(0)=1, \theta(0)=1, \phi(0)=0,\quad f'(\infty)\to 1, \theta(\infty)\to 0, \phi(\infty)\to 0 \tag{13}$$

where

$$A = \frac{\alpha}{c},\ \beta = c\lambda_0,\ \lambda_0 = \frac{\lambda}{1-\alpha t},\ Ha = \sqrt{\frac{\sigma B_0^2}{\rho c}},\ Gr = \frac{g\beta_T(T_w - T_\infty)(1-\alpha t)^2}{c^2 x},\ Sc = \frac{v}{D},\ Gc = \frac{g\beta_c(C_w - C_\infty)(1-\alpha t)^2}{c^2 x},\ \Pr = \frac{v}{\alpha},\ Ec = \frac{c^2 x}{c_p(T_w - T_\infty)(1-\alpha t)^2},\ Nr = \frac{16\sigma^c T_\infty^3}{3k^c k},\ \mathrm{Re}_x = \frac{U_w x}{v} \tag{14}$$

Next are expressions for the skin friction coefficient, heat and mass transfer fluxes at the wall in dimensionless form, these are expressed as:

$$C_f \mathrm{Re}_x^{\frac{1}{2}} = f''(0); \mathrm{Re}^{-1/2} Nu_x = -(1+Nr)\theta'(0); \mathrm{Re}^{-1/2} Sh_x = -\phi'(0) \tag{15}$$

Method of Solution Via Runge-Kutta/Shooting Technique

To apply the Runge-Kutta/Shooting technique, the model Eqs. (10) - (12) together with the boundary conditions (13) are converted to a set of first order initial value problems. Let,

$$y_1 = f,\ y_2 = f',\ y_3 = f'',\ y_4 = \theta,\ y_5 = \theta',\ y_6 = \phi,\ y_7 = \phi' \tag{16}$$

Then in view of Eq. (16), Eqs. (10)-(13) assume the form:

$$\left.\begin{aligned}
&y_1' = y_2,\ y_1(0) = 0\\
&y_2' = y_3,\ y_2(0) = 1\\
&y_3' = \frac{1}{(1-\beta y_1^2)}\Big[y_1 y_3 - y_2^2 + A\left(\frac{\eta}{2} y_3 + y_2\right) + 2\beta y_1 y_2 y_3\\
&\quad -Ha^2(y_2 + \beta y_1 y_3) + (Gr y_4 + Gc y_6)\cos\gamma\Big] y_3 = L_1\\
&y_4' = y_5,\ y_4(0) = 1\\
&y_5' = -\left(\frac{\Pr}{1+Nr}\right)\Big[y_1 y_4 - y_2 y_4 - A\left(\frac{\eta}{2} y_5 + y_4\right)\\
&\quad +Ec\left(y_3^2 + Ha^2 y_2^2\right)\Big],\ y_5(0) = L_2,\\
&y_6' = y_7,\ y_6(0) = 1,\\
&y_7' = -Sc\left[y_1 y_6 - y_2 y_6 - A\left(\frac{\eta}{2} y_7 + y_6\right)\right],\ y_7(0) = L_3
\end{aligned}\right\} \tag{17}$$

The fourth-order Runge-Kutta method is employed on Maple 18 see Rana and Shukla [46] and El-Aziz and Nabil [47] for more on MAPLE software) to obtain the solutions to Eqs (17). A step size of 0.001 is used to calculate the equations' solutions. At a distance where the influence of boundary layers is less substantial, the results are truncated. To verify the validity of the current numerical method, the results have been compared to previously published works in the literature. Thus, in Tables 1, 2 and 3 the results are compared with Grubka and Bobba [18], Ishak [17], Sharidan et al. [19] and Chamkha et al. [20] respectively. In all these, the results demonstrate excellent agreement.

Results and Discussion

Transient MHD Maxwell fluid flow over a stretching surface with thermal radiation, viscous dissipation and Ohmic heating effects has been investigated. For some dimensionless physical values, computed results are presented in Tables 1-3 and Figs. 2-10. The values of the pertinent flow parameters are fixed throughout the analysis except otherwise stated in the figures and tables. These are $A=1$, $\beta=0.1$, $Nr=0.1$, $Gr=1$, $Gc=1$, $\gamma=\pi/6$, $Sc=0.62$, $\Pr=1$, $Ha=0.5$, $Ec=0.1$, $f_w=0$.

Table 1: Comparison of $-\theta'(0)$ for various values of A, H, $\Pr$ for $\beta=0$, $\gamma=90^0$

A	H	$\Pr$	Grubka and Bobba [18]	Ishak [17]	Present
0	0	0.01	0.0197	0.0197	0.1122
		0.72	0.8086	0.8086	0.8088364017
		1	1.0000	1.0000	1.0000083024
		3	1.9237	1.9237	1.9236723873
		6.7		3.0003	3.0002573873
		10	3.7207	3.7207	3.7206520234
		100	12.2940	12.2940	12.294080769

	1	0.01	0.0140	0.1092151587
		0.7	0.68967	0.6915395368
		1	0.8921	0.8924194639
		10	3.6170	3.6169754359
		100	12.194	12.194108365
1	0	0.7	1.0834	1.0833883410
		7	3.7682	3.7682403394
	1	0.7	1.0500	1.0499871879
		7	3.7164	3.7164750608

Table 2: Comparison of $-f''(0)$ with Sharidan et al. and Chamkha et al. [20] $\beta=0, H=0, \gamma=90^0, \mathrm{Pr}=1$

A	Sharidan et al. [19]	Chamkha et al.[20]	Present
0.8	1.261042	1.261512	1.2610468
1.2	1.377722	1.378052	1.3777344

Table 3: Comparison of $-f''(0)$, $-\theta'(0)$ and $-\phi'(0)$ for various values of A, Pr and Sc at $\gamma=1$, $K/H=1$, $Gr=1$, $Gc=2$, $f_w=0.5$

			Chamkha et al. [20]			Present		
A	Pr	Sc	$-f''(0)$	$-\theta'(0)$	$-\phi'(0)$	$-f''(0)$	$-\theta'(0)$	$-\phi'(0)$
0	0.71	0.22	0.27377	1.158393	0.74014	0.273514	1.157477	0.739461
		0.60	0.49677	1.101087	1.312248	0.496533	1.100159	1.311761
		0.94	0.59941	1.076931	1.713443	0.599134	1.076292	1.713094
	0.3	0.62	0.38639	0.62198	1.355045	0.386548	0.621810	1.354616
	0.71		0.50438	1.099032	1.337571	0.505057	1.098321	1.337270
	1		0.55244	1.384875	1.331027	0.552362	1.394657	1.330859
	3		0.69042	2.966999	1.316710	0.690086	2.965405	1.316382
0	0.71	0.62	0.50438	1.099032	1.337571	0.504057	1.098321	1.337270
1			0.88473	1.324178	1.496687	0.884328	1.323532	1.496483
2			1.215097	1.526933	1.648849	1.214068	1.526815	1.648229
10			2.830195	2.656791	2.599922	2.829416	2.656700	2.599545

Figures 2a, 2b and 2c indicate a reduction in fluid velocity near the wall while a rise is registered away from the wall. The momentum and thermal boundary layer thicknesses as well as mass transfer rate decrease as depicted by the plots, which causes the reduction in fluid velocity, temperature, and concentration. In addition, the unsteadiness parameter is a function of fluid thermal diffusivity, that is, $A=\alpha/c$. Increasing the unsteadiness parameter, the fluid thermal diffusivity increases, hence the velocity, temperature and concentration profiles decrease. It is further observed that an opposing trend is displayed in the figures for the free stream region. Next is the influence of inclination parameter (γ), fluid motion is lessened while the temperature and concentration profiles receive a boost as displayed in Fig. 3. Varying the inclination angle as $10^\circ, 45^\circ, 75^\circ$ reduces the impact of gravitational force on the flow, resulting in a drastic reduction in buoyancy force effect, hence the reduction in the fluid motion. This can be compared to when the stretching sheet is vertically downward at $\gamma=0^\circ$, which allows the maximum impact of gravitational force and fluid maximum flow motion. However, fluid temperature and concentration profiles increase due to thermal and concentration boundary layer thicknesses.

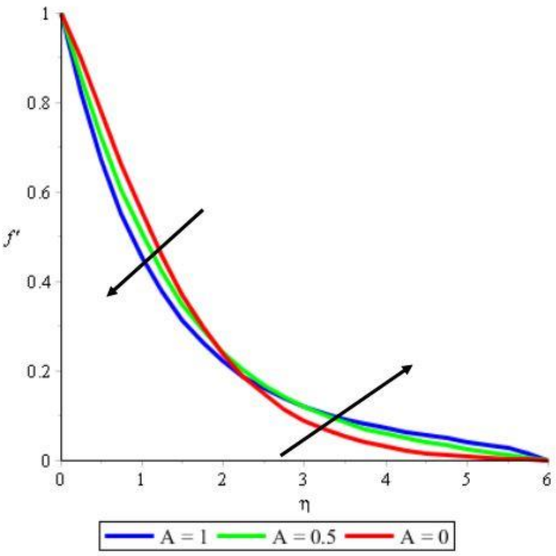

Fig. 2a Velocity, for various values of A

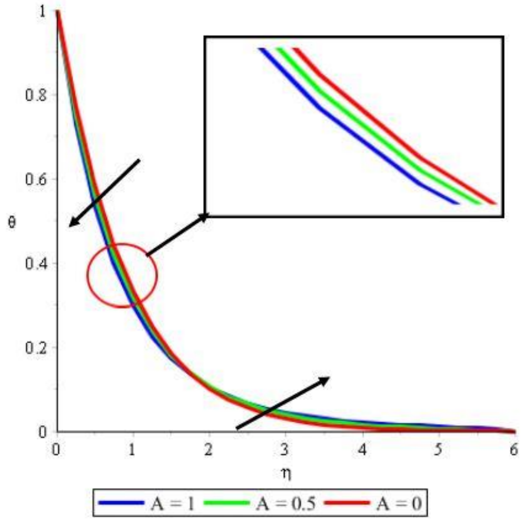

Fig. 2b Temperature for various values of A

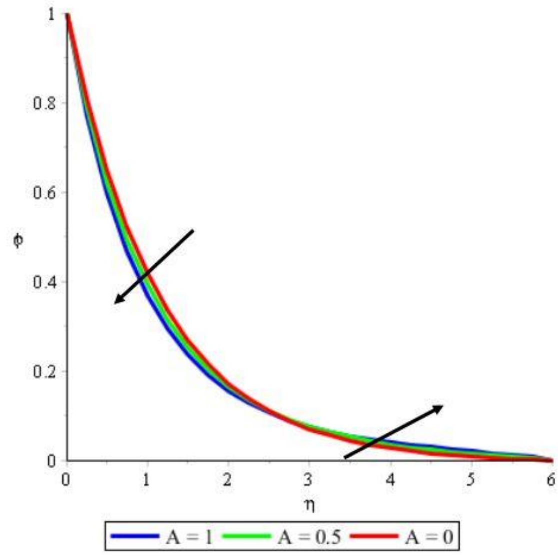

Fig. 2c Concentration for various values of A .

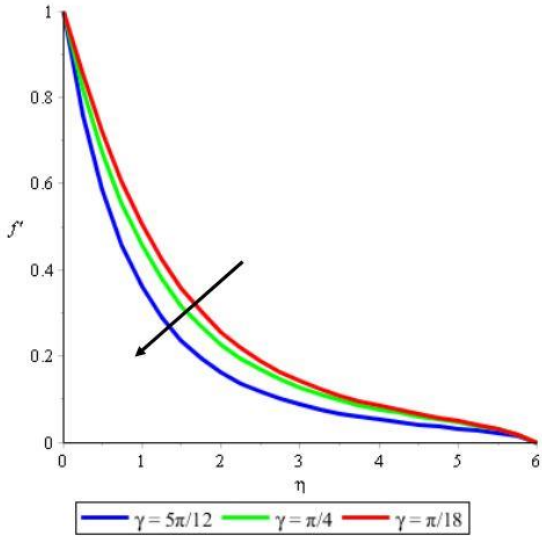

Fig. 3a Velocity for various values of

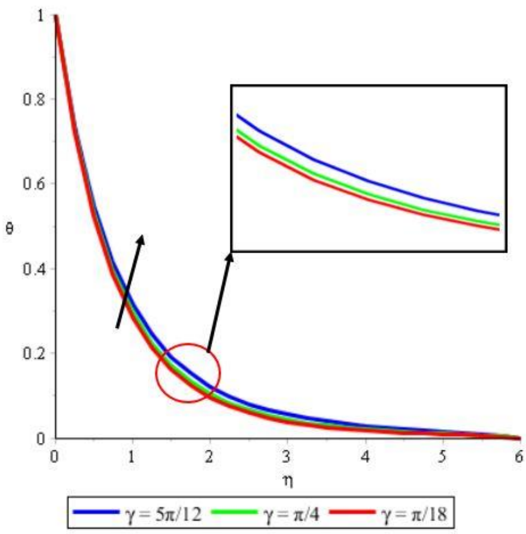

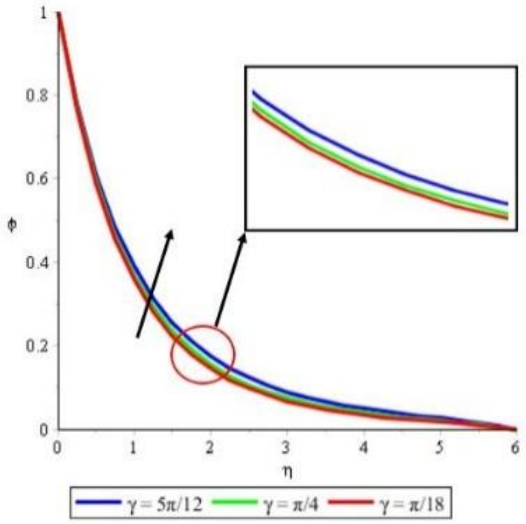

Fig. 3b Temperature for various values of γ

Fig. 3c Concentration for various values of γ

Response of velocity, temperature and concentration profiles to variation in radiation parameter is presented in Figs. 4a, b and c. An increment in fluid velocity and temperature is noticed while fluid concentration is lowered. This happens as a consequence of a decrease in the mean absorption coefficient, k^c as the radiation parameter $Nr\left(=16\sigma^C T_\infty^3/3k^C k\right)$ receives a boost. Consequently, the fluid's rate of radiative heat transfer is rising, leading to a decline in fluid velocity and temperature. However mass concentration is lowered due to a reduction in concentration boundary layer thickness.

Figures 5 and 6 depict the effects of Grashof numbers (Gr , Gc -thermal and concentration buoyancy forces, respectively) on fluid velocity, temperature and concentration profiles. Since Grashof number expresses the buoyant-to-viscous force ratio, physically speaking, $Gr > 0$ denotes heating of the fluid or cooling of the wall, whereas $Gr < 0$ implies cooling of the fluid or heating of the sheet surface. Therefore, increasing the values of Grashof numbers reduces fluid viscosity. This in effect raises fluid motion but cools the fluid temperature and concentration profiles.

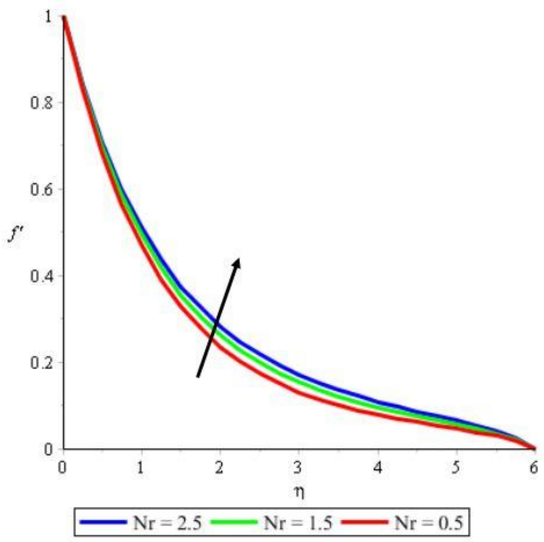

Fig. 4 Velocity for various values of Nr

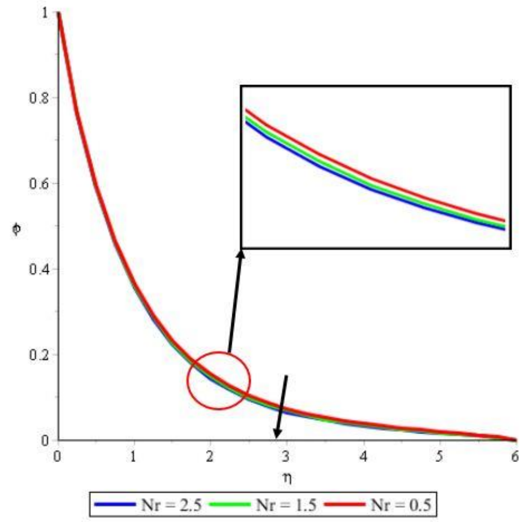

Fig. 4c Concentration (c) for various values of Nr .

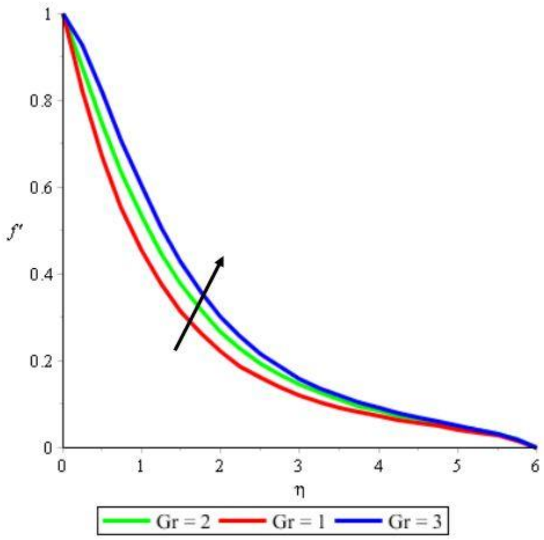

Fig. 5a Velocity for various values of Gr .

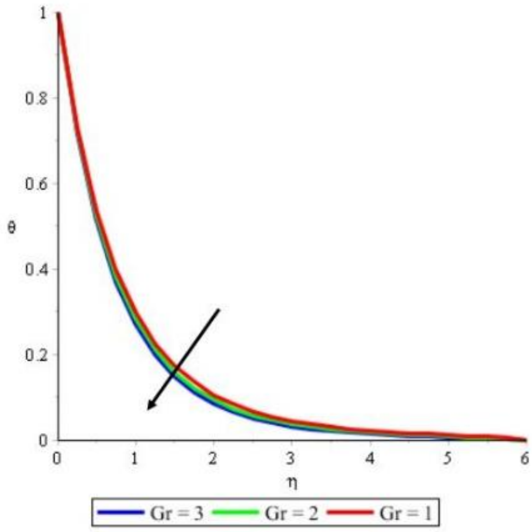

Fig. 5b Temperature for various values of Gr .

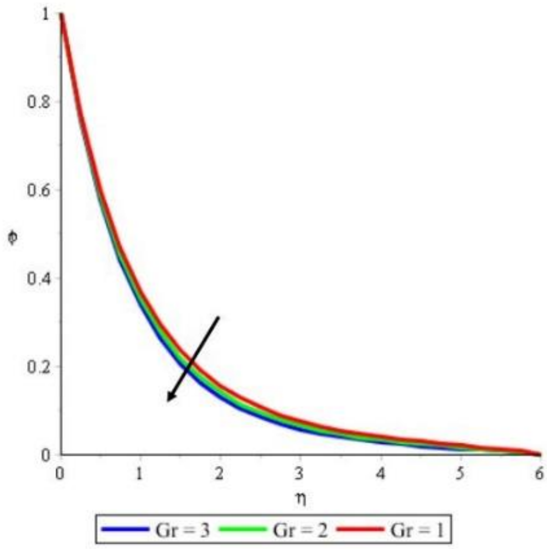

Fig. 5c Concentration for various values of Gr .

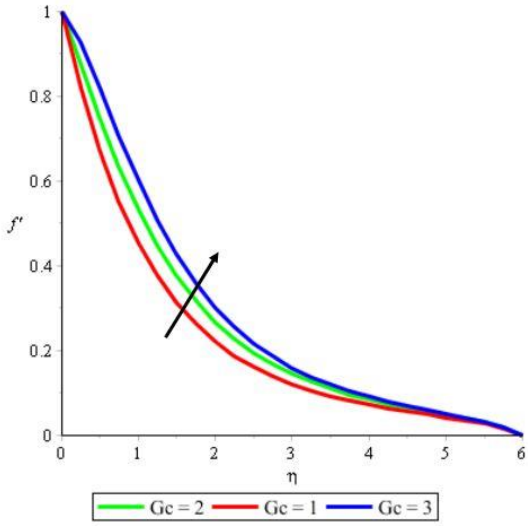

Fig. 6a Velocity for various values of Gc .

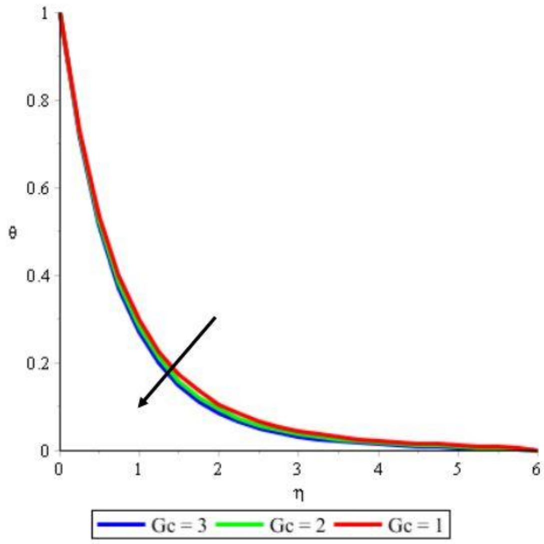

Fig. 6b Temperature for various values of Gc .

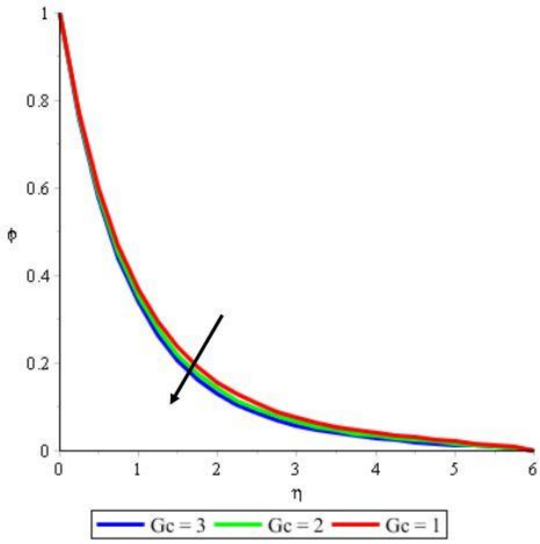

Fig. 6c Concentration for various values of Gc .

In Fig. 7, magnetic field parameter effects on fluid velocity, temperature and concentration are respectively displayed. Fluid velocity drops as the magnetic field parameter value is enhanced. An opposing Lorentz force is generated in an electrically conducting fluid when a magnetic field in a transverse direction to the flow is introduced. As the magnetic field value increases, the fluid velocity decreases as a result of this resistive force's tendency to slow the flow, as displayed in Fig. 7a. However, in Figs. 7b and 7c, an increase is observed in fluid temperature and concentration. This is because Ohmic heating (or Lorentz heating resulting from a magnetic field), which is present in the energy equation, acts as an additional heat source for the flow system, raising the fluid's temperature.

As depicted in Fig. 8, Prandtl number variation has a significant impact on fluid velocity, temperature and concentration profiles. It is observed that a reduction in fluid velocity and temperature is registered while species concentration is enhanced. Physically speaking, this is correct since Prandtl number relates fluid momentum diffusivity to thermal diffusivity. Increasing the value of the Prandtl number from 0.71 to 2 leads to a drop in fluid motion. This is due to a reduction in momentum boundary layer thickness, hence the momentum diffusivity, leading to a reduction in fluid velocity as depicted in Fig. 8a. Furthermore, in Fig. 8b fluid temperature is observed to have significantly reduced. There is a massive increase in fluid thermal conductivity for smaller values of Prandtl number. Therefore, more heat diffuses away from the sheet for reducing values of Prandtl than for its increment. However, species concentration is observed to have improved, as displayed in Figure 8c.

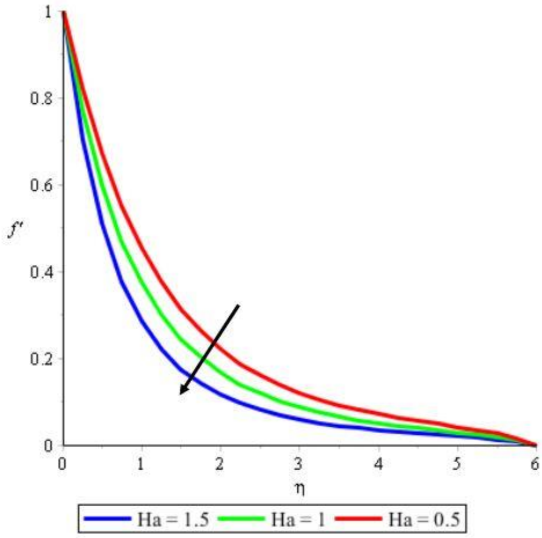

Fig. 7a Velocity for various values of Ha .

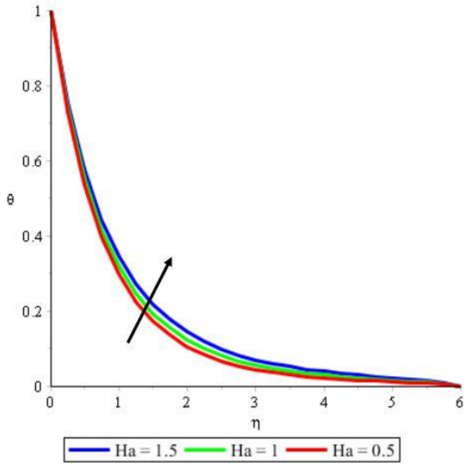

Fig. 7b Temperature for various values of Ha .

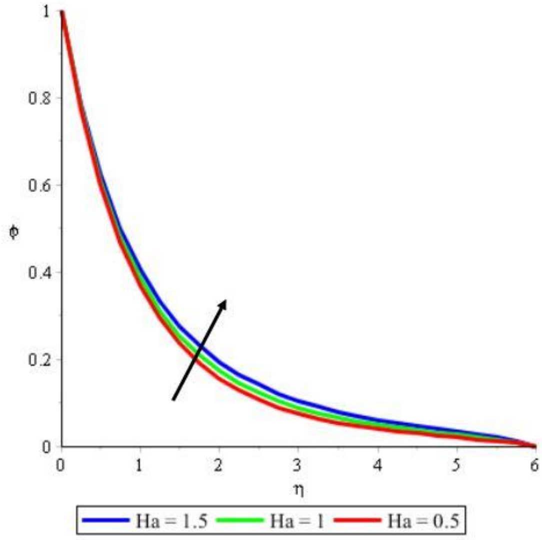

Fig. 7c Concentration for various values of Ha .

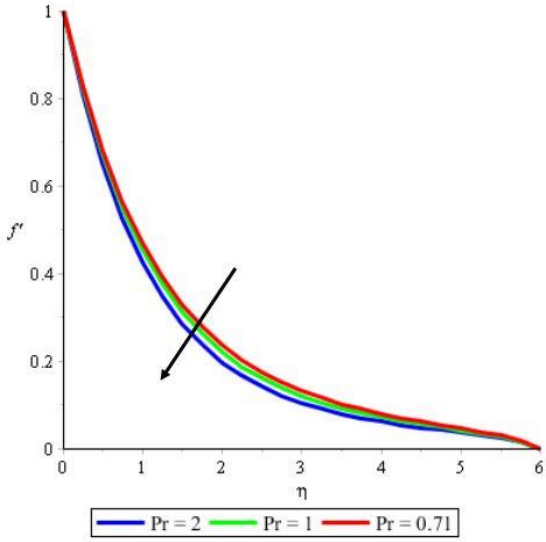

Fig. 8a Velocity for various values of $\Pr$.

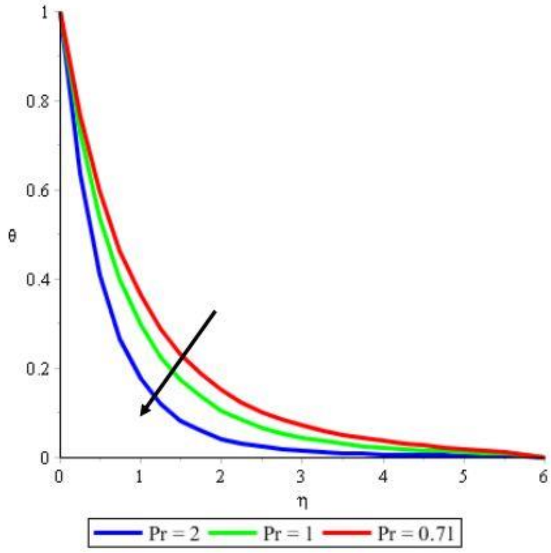

Fig. 8b Temperature for various values of Pr .

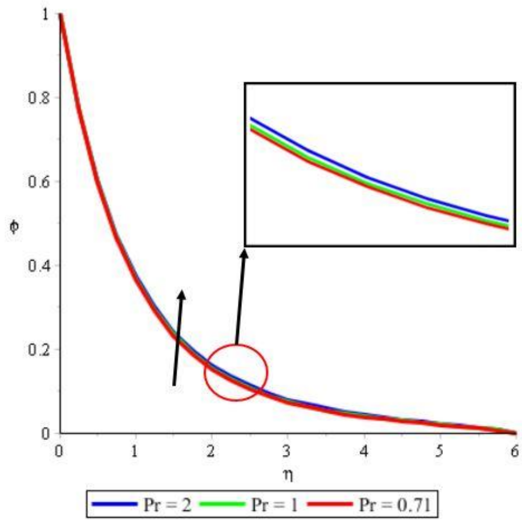

Fig. 8c Concentration for various values of Pr .

The Eckert number improves fluid velocity and temperature while the concentration profile is reduced, as displayed in Fig. 9. Eckert number describes the interaction between the fluid's enthalpy and kinetic energy in the flow. It depicts the process by which kinetic energy is transformed into internal energy as a result of work done against viscous fluid stresses. Therefore, fluid velocity and temperature increase while concentration boundary layer thickness decreases as viscous dissipative heat increases. In Fig. 10, fluid motion and species concentration are observed to have reduced while the temperature increases as Schmidt number is enhanced. The relationship between fluid kinematic viscosity and mass diffusivity is the quantity that is designated as Schmidt number (Sc) in the concentration equation. It explains the association between the relative thickness of the mass-transfer boundary layer and the hydrodynamic boundary layer. Consequently, a rise in the Schmidt number renders the fluid more viscous, resulting in a reduction in fluid motion and concentration while the temperature is raised.

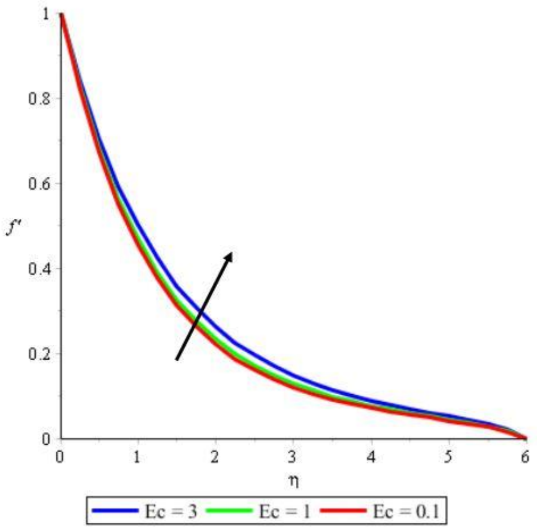

Fig. 9a Velocity for various values of Ec .

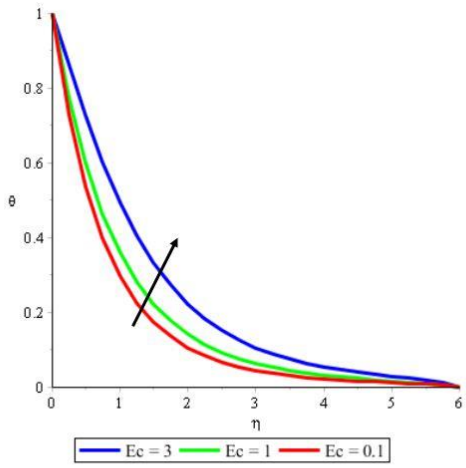

Fig. 9b Temperature for various values of Ec .

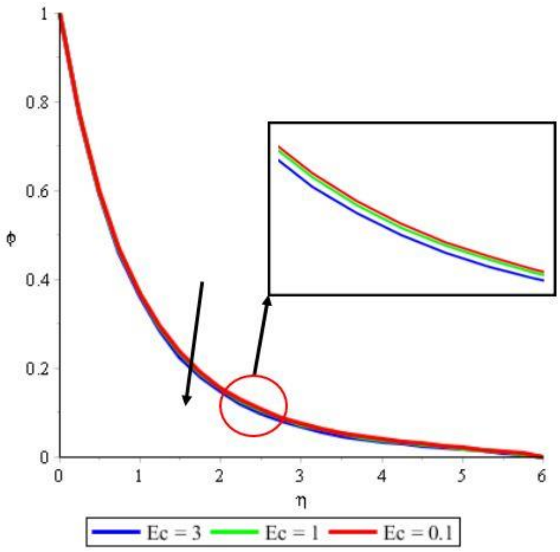

Fig. 9c Concentration for various values of *Ec* .

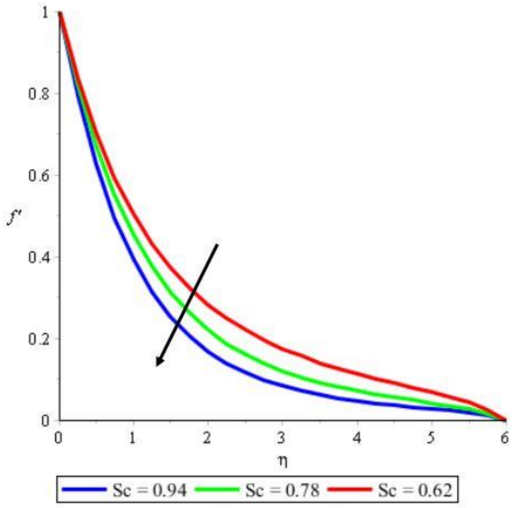

Fig. 10a Velocity for various values of *Sc*

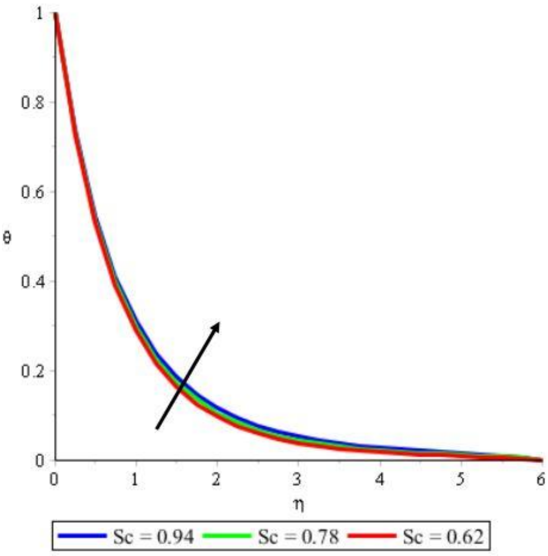

Fig. 10b Temperature for various values of *Sc*

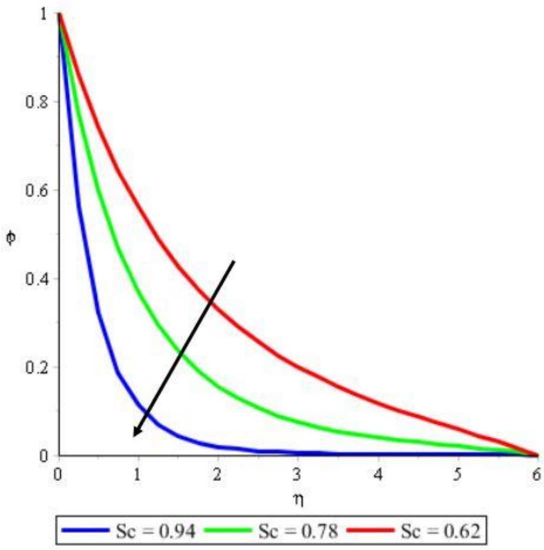

Fig. 10c Concentration for various values of *Sc*

CONCLUSIONS

The current study presents the electrically conducting two-dimensional Maxwell fluid flow through a stretching sheet. Viscous dissipation, inclination angle, Ohmic heating and unsteadiness parameter are incorporated in the optically dense fluid. By applying Runge-Kutta/Shooting technique, numerical solutions are obtained for the ordinary differential equations. Comparing the current findings with the literature that is already available, it is demonstrated that there is good agreement. The following are the key findings:

- Flow motion is decelerated by inclination angle, magnetic field parameters and Prandtl number. However, radiation parameter, Grashof and Eckert numbers accelerated it,
- Fluid temperature is heightened by inclination, radiation and magnetic field parameters. However, Grashof and Prandtl numbers cool the system,
- Concentration of species is enhanced by inclination angle parameter, magnetic field parameter and Prandtl number,
- Heat transfer rate is enhanced by Prandtl number and unsteadiness parameter.

ACKNOWLEDGEMENTS

NOMENCLATURE

a, b, c constants
A unsteadiness parameters
B_0^2 uniform transverse magnetic field
C_p specific heat of the fluid at constant temperature (J/kg·K)
C_w concentration of sheet surface
C_∞ free-stream concentration
D coefficient of mass diffusivity
Ec Eckert number
f dimensionless stream function
g *acceleration due to gravity*
Gr local Grashof number due to temperature differences
Gc local Grashof number due to concentration differences
Ha^2 Hartman number
k thermal conductivity (W/m·K)
k^c absorption coefficient
Nr radiation parameter
Pr Prandtl number
q_r Relative heat flux
Re Local Reynolds number
T temperature of the fluid (K)
T_w temperature of the sheet surface
T_∞ free-stream temperature
Sc Schmidt number
u velocity component along *x* direction
v velocity component along *y* direction

Greek Symbols

α^c thermal diffusivity
β Maxwell parameter
β_c solutal expansion coefficient
β_T thermal expansion coefficient
γ inclination angle
η similarity variable
θ dimensionless temperature
λ relaxation time parameter of the fluid
λ_0 constant
μ dynamic viscosity
ν kinematic viscosity
ρ fluid density (kg/m^3)
σ electrical conductivity
σ^c Stefan Boltzmann constant
ψ stream function

REFERENCES

[1]. Ojjela O, Kumar NN (2016) Chemic ally reacting micropolar fluid flow and heat transfer between expanding or contracting walls with ion slip, Soret and Dufour effects. Alexandria

Engineering Journal 55:1683–1694 https://doi.org/10.1016/j.aej.2016.02.026

[2]. Hussain A, Ullah A (2016) Boundary layer flow of a Walter's B fluid due to a stretching cylinder with temperature dependent viscosity. Alexandria Engineering Journal. 55(4):3073–3080. https://doi.org/10.1016/j.aej.2016.07.037

[3]. Gaffar SA, Prasad VR, Reddy EK (2017) Computational study of Jeffrey's non-Newtonian fluid past a semi-infinite vertical plate with thermal radiation and heat generation/absorption. Ain Shams Engineering Journal 8(2):277–294. https://doi.org/10.1016/j.asej.2016.09.003

[4]. Megahed AM (2019) Williamson fluid flow due to a nonlinearly stretching sheet with viscous dissipation and thermal radiation. J Egypt Math Soc 27(12) https://doi.org/10.1186/s42787-019-0016-y

[5]. Prasad VR, Gaffar SA, Beg OA (2015) Non-similar computational solutions for free convection boundary layer flow of a nanofluid from an isothermal sphere in a non-Darcy porous medium. Journal of Nanofluids 4(2):203–213. https://doi.org/10.1166/jon.2015.1149

[6]. Gaffar SA, Prasad VR, Beg OA (2017) Computational study of non-Newtonian Eyring-Powell fluid from a vertical porous plate with Biot number effects. The Journal of the Brazilian Society of Mechanical Sciences and Engineering **39**(7):2747–2765. https://doi.org/10.1007/s40430-017-0761-5

[7]. Gaffar SA, Prasad VR, Reddy EK (2017) Computational study of MHD free convection flow of non-Newtonian tangent hyperbolic fluid from a vertical surface in porous media with Hall/ionslip current and Ohmic dissipation. International Journal of Applied and Computational Mathematics. **3**(2), 859–890.https://doi.org/10.1007/s40819-016-0135-1

[8]. Mehmood R, Nadeem S, Saleem S, Akbar NS (2017) Flow and heat transfer analysis of a Jeffery nanofluid impinging obliquely over a stretched plate. Journal of the Taiwan Institute of Chemical Engineers, **74**, 49–58. https://doi.org/10.1016/j.jtice.2017.02.001

[9]. Aliakbar A, Pahlavan AA, Sadeghy K (2009) The influence of thermal radiation on MHD flow of Maxwellian fluids above stretching sheets. Communications in Nonlinear Science and Numerical Simulation, **14**, 779–794. https://doi.org/10.1016/j.cnsns.2007.12.003

[10]. _Hayat T, Qasim M (2010) Influence of thermal radiation and Joule heating on MHD flow of a Maxwell fluid in the presence of thermophoresis. International Journal of Heat and Mass Transfer, **53**, 4780-4788. https://doi.org/10.1016/j.ijheatmasstransfer.2010.06.014

[11]. Mukhopadhyay S (2012) Heat transfer analysis of the unsteady flow of a Maxwell fluid over a stretching surface in the presence of a heat source/sink. Chinese Physics Letters, **29** 5. DOI 10.1088/0256-307X/29/5/054703.

[12]. Mukhopadhyay S, Bhattacharyya K (2012) Unsteady flow of a Maxwell fluid over a stretching surface in presence of chemical reaction. Journal of the Egyptian Mathematical Society, **20**, 229–
2 34. https://doi.org/10.1016/j.joems.2012.08.019

[13]. Altan T, Oh S, Gegel H (1979) Metal Forming Fundamentals and Applications. American Society of Metals, Metals Park.

[14]. Fisher FG (1976) Extrusion of Plastics. Wiley New York.

[15]. Tadmor Z, Klein I (1970) Engineering principles of plasticating extrusion, Polymer Science and Engineering Series. Van Nostrand Reinhold New York.

[16]. Crane LJ (1970) Flow past a stretching plate. Zeitschrift für angewandte Mathematik und Physik (ZAMP), **21**, 645–647. https://doi.org/10.1007/BF01587695

[17]. Ishak A (2010) Unsteady MHD and Heat Transfer over a stretching Plate. Journal of Applied Sciences, **10**(18), 2127-2131. https://scialert.net/abstract/?doi=jas.2010.2127.2131

[18]. Grubka LJ, Bobba KM (1985) Heat transfer characteristics of a continuous, stretching surface with variable temperature. Journal of Heat Transfer. **107:**248-250. https://doi.org/10.1115/1.3247387

[19]. Sharidan S, Mahmood T, Pop I (2006) Similarity solutions for the unsteady boundary layer flow and heat transfer due to a stretching sheet. International Journal of Applied Mechanics **11**:647–654.

[20]. Chamkha AJ, Aly AM, Mansour MA (2010) Similarity solution for unsteady heat and

mass transfer from a stretching surface embedded in a porous medium with suction/injection and chemical reaction effects. Chemical Engineering Communications, **197**(6):846-858. https://doi.org/10.1080/00986440903359087
[21]. Eldabe NTM, Elsaka AG, Radwan AE, Eltaweel MAM (2010) Three-dimensional flow over a stretching surface in a viscoelastic fluid with mass and heat transfer. Nature and Science Journal, 8(8):218-228. http://www.dx.doi.org/10.7537/marsnsj080810.26
[22]. Yusuf TA, Adesanya SO, Gbadeyan JA (2020) Entropy generation in MHD Williamson nanofluid over a convectively heated stretching plate with chemical reaction. Heat Transfer 1–18. http://dx.doi.org/10.32604/cmc.2020.012505
[23]. Mustafa M, Hayat T, Pop I, Aziz A (2011) Unsteady boundary layer flow of a Casson fluid due to an impulsively started moving flat. Heat Transfer Asian Research **40**:563-557. http://dx.doi.org/10.1002/htj.20358
[24]. Rosseland S (1931) Astrophysik und atom-theoretische Grundlagen. Springer Verlag, Berlin 41–44. https://doi.org/10.1007/978-3-662-26679-3
[25]. Hossain MA, Takhar HS (1996) Radiation effects on mixed convection along a vertical plate with uniform surface temperature. Heat Mass Transfer **31**: 243-248. https://doi.org/10.1007/BF02328616
[26]. Hossain MA, Alim MA, Rees D (1999) The effect of radiation on free convection from a porous vertical plate. International Journal of Heat and Mass Transfer, **42**, 181-191. https://doi.org/10.1016/S0017-9310(98)00097-0
[27]. Bataller RC (2008) Radiation effects for the Blasius and Sakiadis flows with a convective surface boundary condition. Applied Mathematics and Computation **206**: 832-840 https://doi.org/10.1016/j.amc.2008.10.001
[28]. Sajid M, Hayat T (2008) Influence of thermal radiation on the boundary layer flow due to an exponentially stretching sheet. International Communications in Heat and Mass Transfer. **35,** 347-356. https://doi.org/10.1016/j.icheatmasstransfer.2007.08.006
[29]. Gbadeyan JA, Yusuf TA (2019) Effect of nonlinear partial slip and thermal radiation on Oldroyd 8 ‐ constant fluid in a channel with convective boundary condition. Heat Transfer, **49**(2):755-778. https://doi.org/10.1002/htj.21637
[30]. Makinde OD (2010) MHD mixed-convection interaction with thermal radiation and nth order chemical reaction past a vertical porous plate embedded in a porous medium. Chemical Engineering Communications, **198**(4):590–608. https://doi.org/10.1080/00986445.2010.500151
[31]. Vajravelu K, Hadjinicolaou A (1993) Heat transfer in a viscous fluid over a stretching sheet with viscous dissipation and internal heat generation. International Communications in Heat and Mass Transfer **20**(3):417-430. https://doi.org/10.1016/0735-1933(93)90026-R
[32]. Partha MK, Murthy PVSN, Rajasekhar GP (2005) Effect of viscous dissipation on the mixed convection heat transfer from an exponentially stretching surface. Heat Mass Transfer 41(4):360-366. https://doi.org/10.1007/s00231-004-0552-2
[33]. Sanjayanand E, Khan SK (2006) On heat and mass transfer in a viscoelastic boundary layer flow over an exponentially stretching sheet. International Journal of Thermal Sciences **45**(8): 819-828. https://doi.org/10.1016/j.ijthermalsci.2005.11.002
[34]. Cortell R (2008) Effect of viscous dissipation and radiation on the thermal boundary layer over a non-linearly stretching sheet. Physics Letters A **372**(5): 631-636. https://doi.org/10.1016/j.physleta.2007.08.005
[35]. Aziz EMA (2009) Viscous dissipation effect on mixed convection flow of a micropolar fluid over an exponentially stretching sheet. Canadian Journal of Physics **87**(4):359-368. https://doi.org/10.1139/P09-047
[36]. Pavithra GM, Gireesha BJ (2013) Effect of viscous dissipation on hydromagnetic fluid flow and heat transfer in a porous medium at an exponentially stretching sheet with fluid particle suspension. Afrika Matematika, **26**:419-432. https://doi.org/10.1007/S13370-013-0214-Y
[37]. Anjali Devi SP, Ganga B (2009) Effects of viscous and joules dissipation on MHD flow, heat and mass transfer past a stretching porous surface embedded in a porous medium. Nonlinear Analysis: Modelling and Control 14(3):303–314. https://doi.org/10.15388/NA.2009.14.3.14497
[38]. Megahed AM (2019) Carreau fluid flow due to nonlinearly stretching sheet with thermal radiation,

heat flux, and variable conductivity. Applied Mathematics and Mechanics **40**:1615–1624. https://doi.org/10.1007/s10483-019-2534-6

[39]. Swain BK, Parida BC, Kar S, Senapati N (2020) Viscous dissipation and joule heating effect on MHD flow and heat transfer past a stretching sheet embedded in a porous medium Heliyon 6(10), https://doi.org/10.1016/j.heliyon.2020.e05338

[40]. Muhammad T, Hayat T, Shehzad SA, Alsaedi A (2018) Viscous dissipation and Joule heating effects in MHD 3D flow with heat and mass fluxes. Results in Physics **8**:365-371. https://doi.org/10.1016/j.rinp.2017.12.047

[41]. Adegbie KS, Samuel DJ, Ajayi BO (2019) Ohmic heating of Magnetohydrodynamic viscous flow over a continuous moving plate with viscous dissipation buoyancy and thermal radiation. Defect Diffusion Forum **392**:73-91.

[42]. Osalusi E, Side J, Harris R (2007) The effects of Ohmic heating and viscous dissipation on unsteady MHD and slip flow over a porous rotating disk with variable properties in the presence of Hall and ion-slip currents. International Communications in Heat and Mass Transfer **34**(9-10):1017-1029. https://doi.org/10.1016/j.icheatmasstransfer.2007.05.009

[43]. Goud BS, Nandeppanavar MM (2021) Ohmic heating and chemical reaction effect on MHD flow of micropolar fluid past a stretching surface. Partial Differential Equations in Applied Mathematics, **4** https://doi.org/10.1016/j.padiff.2021.100104

[44]. Hasan MM, Samad MA, Hossain MA (2020) Effects of Hall Current and Ohmic Heating on Non-Newtonian Fluid Flow in a Channel due to Peristaltic Wave. Applied Mathematics-a Journal of Chinese Universities Series B, **11**:292-306. https://doi.org/10.4236/am.2020.114022

[45]. Gireesha BJ, Ganesh Kumar K, Krishnamurthy MR Manjunatha S, Rudraswamy NG (2019) Impact of Ohmic heating on MHD mixed convection flow of Casson fluid by considering Cross diffusion effect. Nonlinear Engineering, 8(1):380-388. https://doi.org/10.1515/nleng-2017-0144

[46]. Rana P, Shukla N (2018) Entropy generation analysis for non-similar analytical study of nanofluid flow and heat transfer under the influence of aligned magnetic field," *Alexandria Engineering Journal*, **57**(4), 3299-3310. https://doi.org/10.1016/j.aej.2017.12.007

[47]. El-Aziz M.A, Nabil T (2012) Homotopy Analysis Solution of Hydromagnetic Mixed Convection Flow Past an Exponentially Stretching Sheet with Hall Current. Mathematical Problems in Engineering. https://doi.org/10.1155/2012/454023